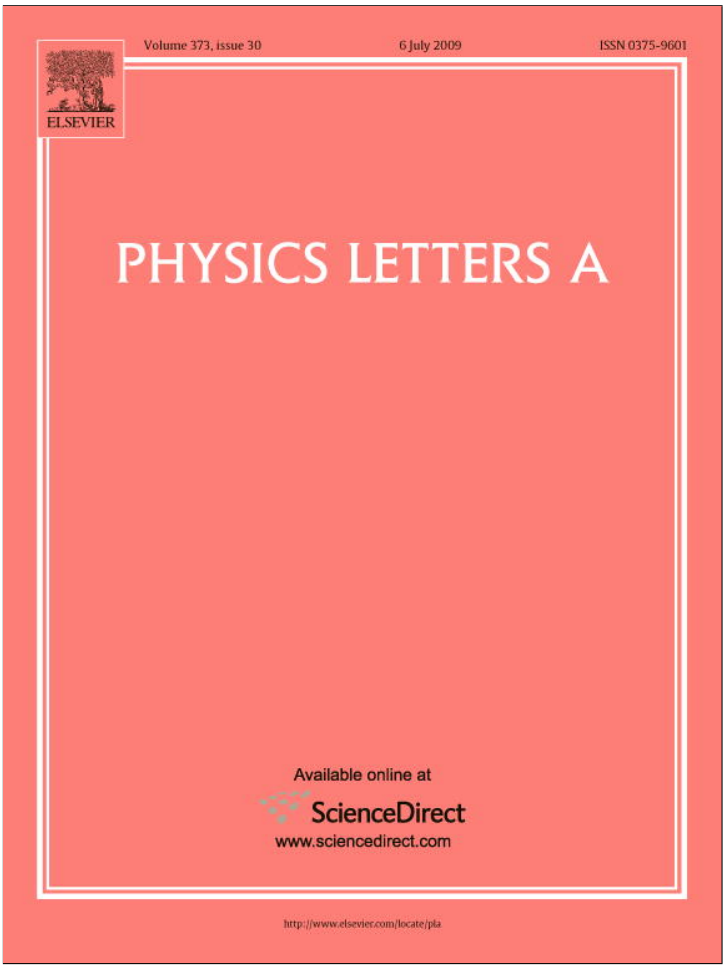

Physics Letters A 373 (2009) 2568–2571

Contents lists available at ScienceDirect

Physics Letters A

www.elsevier.com/locate/pla

Effect of cathode structure on neutron yield performance of a miniature plasma focus device

Rishi Verma [a,1], R.S. Rawat [a,*], P. Lee [a], S. Lee [a], S.V. Springham [a], T.L. Tan [a], M. Krishnan [b]

[a] NSSE, National Institute of Education, Nanyang Technological University, 1 Nanyang Walk, Singapore-637616, Singapore
[b] Alameda Applied Sciences Corporation, San Leandro, CA 94577, USA

ARTICLE INFO

Article history:
Received 19 February 2009
Received in revised form 4 May 2009
Accepted 15 May 2009
Available online 23 May 2009
Communicated by F. Porcelli

PACS:
52.58.Lq
29.25.Dz
82.80.Rt
85.60.Ha

Keywords:
Miniature plasma focus
Neutrons
Time of flight
Pinch current

ABSTRACT

In this Letter we report the effect of two different cathode structures – tubular and squirrel cage, on neutron output from a miniature plasma focus device. The squirrel cage cathode is typical of most DPF sources, with an outer, tubular envelope that serves as a vacuum housing, but does not carry current. The tubular cathode carries the return current and also serves as the vacuum envelope, thereby minimizing the size of the DPF head. The maximum average neutron yield of $(1.82 \pm 0.52) \times 10^5$ n/shot for the tubular cathode at 4 mbar was enhanced to $(1.15 \pm 0.2) \times 10^6$ n/shot with squirrel cage cathode at 6 mbar operation. These results are explained on the basis of a current sheath loading/mass choking effect. The penalty for using a non-transparent cathode negates the advantage of the smaller size of the DPF head.

A long-standing problem of plasma focus devices has been to elucidate the mechanism of neutron production and the correlation between various factors that influence the neutron yield. Over the past few decades various attempts have been made to enhance the neutron yield from deuterium plasma focus devices, for their probable use in fast-neutron activation analysis (FNAA) applications [1], by optimizing various parameters such as anode geometry [2], anode material [3], insulator sleeve material and length [4,5], centre electrode polarity [6], radioactivity assisted pre-ionization [7,8] and high-atomic number gas admixture concentration [9].

Recently many groups have reported the development of miniature plasma focus devices as portable neutron sources [10–15]. A potential limitation of such miniature sources is the fact that the neutron output tends to scale roughly as $(\text{current})^4$ or as $(\text{stored energy})^2$. Hence as one scales down to the sub-kilojoule range (with <100 kA currents) there is a premium on finding ways in which to increase the neutron output above the observed, unfavorable scaling criteria. Among these options is to vary the cathode geometry, which is the province of this Letter. The influence of cathode structure on neutron emission is an important issue since in the typical miniature plasma focus devices, the conventional bar/squirrel cage cathodes are replaced with tubular cathodes [10,11] that double as vacuum barriers and hence reduce the size of the DPF "head". However, the price for this miniaturization in term of its effects on neutron yield has not been investigated; hence in this Letter we describe the effect of conventional squirrel cage cathode structure as opposed to that of newly adopted tubular cathode structure on the neutron yield.

We present results from two different types of cathode geometries (whilst maintaining other operating conditions/parameters and varying only the pressure to optimize the neutron output) on neutron emission from newly developed fast miniature plasma focus device – FMPF-1 [9,10].

The capacitor bank of the FMPF-1 consists of four 0.6 μF, 30 kV capacitors in a compact layout. The detailed design and characterization of this device have been described elsewhere [10]. In the present arrangement, the optimized electrode assembly consists of a 15 mm long stainless steel hollow anode of composite geometry (tapered over the last 5 mm with diameter decreasing from 12 mm to 7 mm) and the cathode diameter is 30 mm. These electrode as-

* Corresponding author.
E-mail address: rajdeep.rawat@nie.edu.sg (R.S. Rawat).
[1] Also at: Pulsed Power Group, Institute for Plasma Research, Bhat, Gandhinagar, Gujarat 382428, India.

0375-9601/$ – see front matter
doi:10.1016/j.physleta.2009.05.025

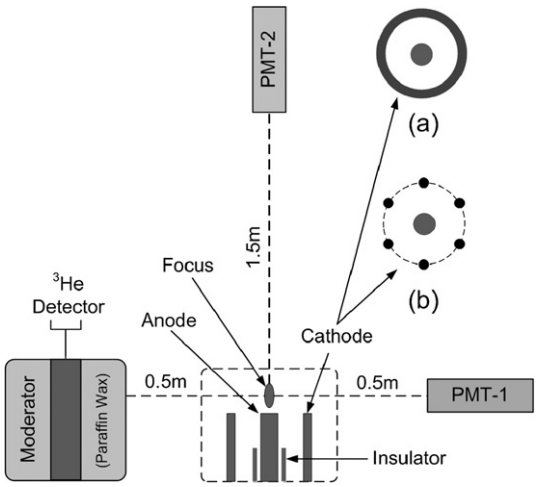

Fig. 1. Layout of time resolved and time integrated neutron diagnostic set-up.

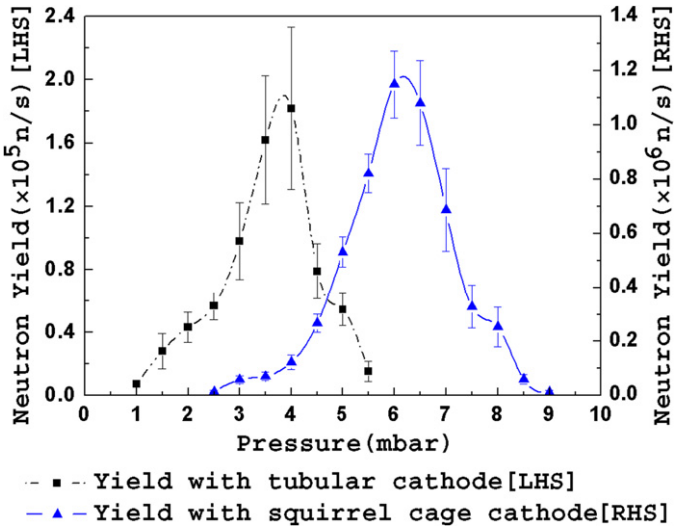

Fig. 2. Neutron yield versus D_2 filling gas pressure for tubular and squirrel cage cathode.

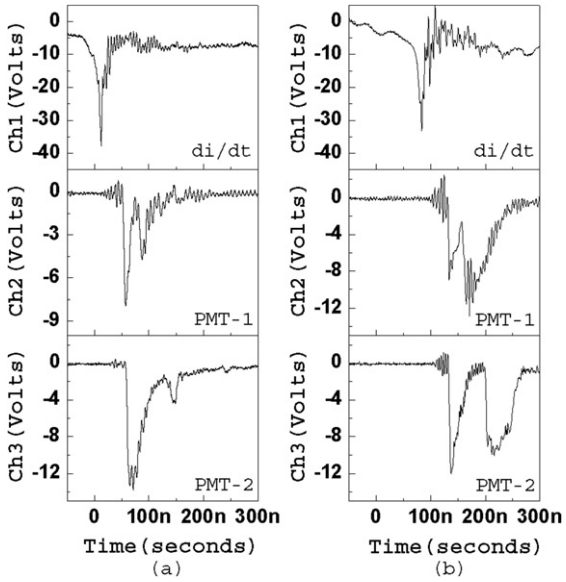

Fig. 3. Current derivative signal trace with HXR/neutron signal recorded with side-on (PMT-1) and end-on (PMT-2) scintillator-photomultiplier detector with (a) tubular cathode, (b) squirrel cage cathode.

sembly dimensions are improved over the dimensions mentioned in our previously published work [10] and they provide better neutron yields as discussed later.

A specially designed Rogowski coil (having response time <3 ns) was used for electrical diagnostics. To measure time integrated neutron yields, a high sensitivity ^{3}He detector arrangement has been used [10,16]. To acquire the time resolved history of emitted radiation, a 'dual time of flight' arrangement consisting of two identical scintillator photomultiplier detectors – PMT-1 and PMT-2 was used. Each of the scintillator photomultiplier detectors consists of an NE102A plastic scintillator (of thickness 40 mm and diameter of 50 mm) and photomultiplier tube EMI 9813B (biased at -1800 V and enclosed inside 1 cm thick Aluminum casing). The PMT-1 was placed radially (90°) at a distance of 0.5 m from the anode face, whereas PMT-2 was placed axially (0°) at a distance of 1.5 m from the anode face along the anode axis. A schematic drawing of this arrangement is shown in Fig. 1. In the insets images of the utilized tubular and squirrel cage cathode structures are shown as inset (a) and inset (b), respectively.

The effects of tubular and squirrel cage cathode geometries on neutron and hard X-ray (HXR) emissions for different fill pressures are investigated at the fixed stored energy of 230 J (with about 80 kA peak discharge current at 13.8 kV charging voltage). The results were obtained for averages of 20 shots for every choice of deuterium gas pressure. To reduce the effect of electrode particulate contamination on neutron output, the gas was refreshed after every five shots. A nominal pressure increase of ≈0.05 mbar was observed after each set of 5 shots.

Our experiments with two different cathode geometries have demonstrated that the final pinch characteristics and in particular, the emission of neutrons is strongly influenced by the cathode structure. The measured average neutron outputs for tubular and squirrel cage cathode geometries, for different D_2 filling gas pressures, are shown in Fig. 2. A remarkable enhancement in neutron yield was observed with squirrel cage cathode operation. The maximum average neutron output of $(1.82 \pm 0.52) \times 10^5$ and $(1.15 \pm 0.2) \times 10^6$ n/shot were measured for tubular and squirrel cage cathode geometries, respectively. It is also observed that the neutron yield peaked at the higher gas pressure 6 mbar for squirrel cage cathode while it peaked at 4 mbar for tubular cathode structure.

Time resolved information about the hard X-ray and neutron emission is obtained using the scintillator photomultiplier detectors PMT-1 and PMT-2 for tubular and squirrel cage cathodes. Those data are shown in Fig. 3 along with corresponding di/dt signals. The first peak in the PMT signals of these two figures (shown as Ch2 and Ch3), is of non-thermal, hard X-rays produced by the instability accelerated electron beam upon hitting the anode target. The second peak is confirmed to be that of neutrons, on the basis of time of flight estimates, assuming that the hard X-rays and neutrons are created at the same time in the pinch. Since the PMT-1 and PMT-2 were placed at a distance of 0.5 m (radially) and 1.5 m (axially), from and along the anode axis, subsequent registration of neutron pulses (i.e. second, delayed peak in the respective signals) at about 23 ± 2 ns and 66 ± 3 ns, respectively, after the emission of hard X-ray pulses confirms that the second peak is due to ≈2.45 MeV D–D neutrons. The relative time difference of 45 ± 3 ns, between the neutron pulses, recorded by the channels Ch2 and Ch3 also re-confirms the neutron pulse emission. The average duration of HXR and neutron pulses, estimated from the FWHM of the corresponding peaks and averaged over 20 shots, in the axial/radial direction are 18 ± 3 ns/12 ± 2 ns and 16 ± 3 ns/16 ± 2 ns, respectively, for tubular cathode operation (Fig. 3(a)), and 18 ± 2 ns/15 ± 2 ns and 46 ± 3 ns/45 ± 2 ns, respectively, for squirrel cage cathode opera-

tion (Fig. 3(b)). The ∼30 ns delay in the appearance of HXR peak (Ch2 and Ch3 trace in the respective figures) from the peak of the current derivative signal (Ch1 trace) is because of the inherent latency in the PMT.

In the plasma focus, the run-down phase allows the transfer of electrical energy from the capacitor bank to the magnetic energy behind the accelerating current sheath a fraction of which is rapidly pumped into the pinch plasma column at the end of radial compression phase in a relatively short time, leading to efficient compression and heating [17]. Under stationary initial gas conditions (unlike in a supersonic gas puff) it is impossible to decouple the final radial compression phase and corresponding plasma phenomena from those occurring during the breakdown and axial run down phases [18]. Therefore, while considering losses in a typical (non-gas-puffed) plasma focus device, the thermal flow down the axis during axial acceleration is an important consideration.

The very high temperature achieved in the plasma focus is mainly the result of the axis-symmetric properties of the imploding shock. Since in the case of the tubular cathode, the outer electrode is an impermeable wall, when there is momentum flowing parallel to the shock, to obtain pressure balance along the shock and near the wall, the plasma density adjacent to the wall must increase. This momentum flowing parallel to the shock thus acts as a sink for the incoming plasma and causes a drop in temperature with increasing radius (as the magnetic pressure falls). With lower temperatures adjacent to the cathode wall and in particular lower electron temperatures, the shock is broadened (with increase in thickness) through resistive diffusion of the magnetic field [19,20]. Aggregation of plasma density near the cathode wall also affects the final temperature that is achieved in the pinch, owing to the fact that compression ratio is mainly dominated by $\rho_{\text{pinch}}/\rho_{\text{shock}}$ and only a partial fraction (about 15%) of the plasma is collected into the ensuing pinch [19]. Hence, in the case of tubular cathodes, due to larger contact area (in comparison with squirrel cage cathode), deleterious effects because of plasma aggregation near the cathode wall are expected to be more pronounced, with a consequent reduction in neutron output.

Another important noticeable observation in the graph shown in Fig. 2 (neutron output vs. filling gas pressure); is the relative shift in the optimum base pressure range with the use of tubular and squirrel cage cathode geometries [21]. The difference in the optimum base pressure range for the two cathode geometries can be explained by the fact that since the geometry of the squirrel cage cathode, allows mass to pass through, during the axial run down phase, the inter-electrode space is relatively clear. In the case of tubular cathodes the outward flow is blocked (due to current sheath canting), then the channel (i.e. the inter electrode space) tends to get constricted due to growing thickness of 'contact layer'. When this layer gets thick enough the channel tends to get loaded/choked. In addition, the outward moving particles are reflected back along with impurities from cathode wall causing substantial increase in thermal bremsstrahlung radiation loss [22] due to impurity addition. In any case, with the use of tubular cathode geometry the cross sectional area of the channel gets effectively reduced, which accounts for loading of current sheath at comparatively lower operating pressure. This observation is corroborated by the measurements shown in Fig. 4, where the variation in time to pinch from the breakdown phase (which includes axial acceleration phase and compression phase, defined as t_p in the current derivative signal shown in the inset), at different filling gas pressures is plotted, for the tubular and squirrel cage cathode geometries. Usually in a typical plasma focus device operation, the characteristic time t_p, increases with the increase in operating pressure due to increased load on the current sheath in the axial phase. In the graph shown, larger slope angle of the operation curve for tubular cathode (by contrast to squirrel cage cathode operation), indicates comparatively higher loading of the current sheath, even at lower pressures. The squirrel cage cathode seems to lessen much of these effects and thus performs with better efficiency resulting in higher yields.

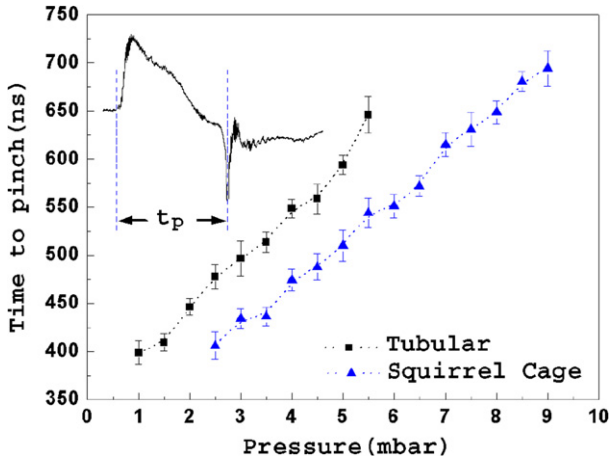

Fig. 4. Time to pinch versus D_2 filling gas pressure for tubular and squirrel cage cathode operation.

Interestingly, it may also be noted that, the 'time to pinch' witnessed for the corresponding cathode geometries (tubular and squirrel cage) at which the neutron yield maximizes is the same i.e. ∼550 ns, while operating at 4 mbar and 6 mbar, respectively. This observation also corroborates the current sheath loading/choking effect with use of tubular cathodes.

Recently, neutron yield scaling has been thoroughly reviewed by S. Lee et al. [23–25], using the five-phase Lee model (RADPFV5.13) [26], and found to follow $Y_n \sim I_{\text{pinch}}^x$ where I_{pinch} is the pinch current that actually participates in the focus pinch phase and x is found to vary in the range of 3–5 for different plasma focus devices. To realistically simulate the experiment using Lee model, firstly the circuit parameters, electrode dimensions, operating voltage and gas pressure are keyed into the code, then the computed current trace is 'fitted' to the experimental peak discharge current trace, by adjusting four 'model parameters'. These four parameters for 'fitting' are axial mass swept-up factor f_m and axial current factor f_c (which characterize axial phase electrodynamics), radial mass factor f_{mr} and radial current factor f_{cr} (which characterize radial phase dynamics). These model parameters are then fine-tuned till the computed trace is in close agreement with the experimentally measured peak discharge current trace [24]. The main objective of using the Lee code is to investigate the changes in the fitting model parameters and electrodynamic behavior for the two cathode geometries to deduce and understand the corresponding changes in plasma dynamics and pinch current. The fine tuned electrical circuit parameters used for the simulation of respective geometries are: 2.4 μF, 32.9 nH and 60 mΩ for tubular cathode operation and 2.4 μF, 31.0 nH and 67 mΩ for squirrel cage cathode operation. A typical 'fitted' trace of squirrel cage cathode operation at 6 mbar gas pressure is shown in Fig. 5. Values of 'model parameters' that have been obtained for 'best fit' with tubular and squirrel cage cathodes (at 4 and 6 mbar, respectively), along with peak/pinch current estimations are summarized in Table 1. The two key differences that can be noticed from Table 1 are (i) for tubular cathode structure, the values of axial mass swept-up factor f_m and radial mass factor f_{mr} are about ∼1.82 and ∼2.2 times higher, respectively, than that obtained for squirrel cage cathode operation which supports the argument and observation of the mass loading of the current sheath for tubular operation and (ii) the estimated pinch current is lower for tubu-

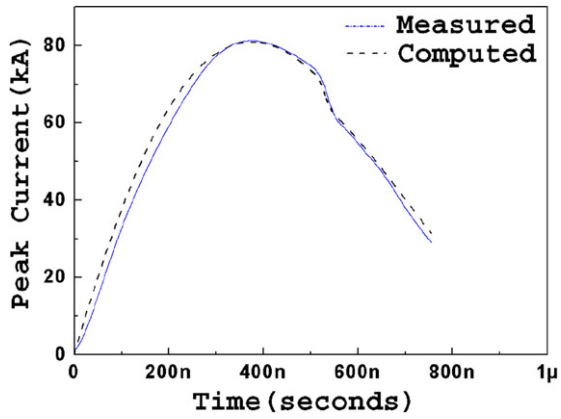

Fig. 5. A "fitted" current trace for squirrel cage cathode operation at 6 mbar filling gas pressure.

Table 1
Model parameters and simulation results

Cathode	f_m	f_{mr}	f_c	f_{cr}	I_{pinch}/I_{peak}
Tubular	0.31	0.33	0.62	0.84	54 kA/81 kA
Squirrel cage	0.17	0.15	0.62	0.89	58 kA/80 kA

lar cathode operation supporting the lower neutron output for this cathode.

In conclusion, our investigation shows a notable enhancement in the neutron output for the squirrel cage geometry as compared to that of a tubular geometry. In a tubular cathode structure, owing to the impermeable wall and relatively larger surface area, the plasma density rises near the cathode wall, causing the shock to be radially broadened through resistive diffusion of the magnetic field. This results in the narrowing of the effective channel cross-section, causing loading of the current sheath along with increased contact layer resistance thereby resulting in lower pinch efficiency. It may also be realized from the Lee model fitting of our experimental results that operation with tubular cathodes also affects the current going out from the main current sheath to the residual plasma as a consequence well-known "current leakage" effect. The fraction of peak discharge current that actually goes from main current sheath to the pinch (i.e. pinch current I_{pinch}) is reduced for tubular cathode operation supporting the lower neutron output for this cathode. Also in operation with tubular cathodes, addition of impurities (due to back reflected particles from the cathode wall) during the axial flow, may result in a substantial drop in temperature due to increased radiation loss which is also consistent with the reduction in neutron output.

Acknowledgements

The authors are grateful to the National Institute of Education/Nanyang Technological University, Singapore, for Scholarship grant and AcRF grant RP 3/06/RSR. One of us, R.V., would like to thank parent organization IPR, Gandhinagar, Gujarat, India for providing study leave to pursue Phd Programme at NTU.

References

[1] V. Gribkov, A. Dubrovsky, L. Karpinski, R. Miklaszewski, M. Paduch, M. Scholz, P. Strzyzewski, K. Tomaszewski, AIP Conf. Proc. 875 (2006) 415.
[2] J.M. Koh, R.S. Rawat, A. Patran, T. Zhang, D. Wong, S.V. Springham, T.L. Tan, S. Lee, P. Lee, Plasma Sources Sci. Technol. 14 (2005) 12.
[3] A. Shyam, R.K. Rout, Phys. Scr. 57 (1998) 290.
[4] F.N. Beg, M. Zakaullah, G. Murtaza, M.M. Beg, Phys. Scr. 46 (1992) 152.
[5] M. Zakaullah, T.J. Baig, S. Beg, G. Murtaza, Phys. Lett. A 137 (1989) 39.
[6] G. Decker, W. Kies, G. Pross, Phys. Lett. A 89 (1982) 393.
[7] M. Zakaullah, A. Waheed, S. Ahmad, S. Zeb, S. Hussain, Plasma Sources Sci. Technol. 12 (2003) 443.
[8] S. Ahmad, S.S. Hussain, M. Sadiq, M. Shafiq, A. Waheed, M. Zakaullah, Plasma Phys. Control. Fusion 48 (2006) 745.
[9] R. Verma, P. Lee, S. Lee, S.V. Springham, T.L. Tan, R.S. Rawat, M. Krishnan, Appl. Phys. Lett. 93 (2008) 101501.
[10] R. Verma, M.V. Roshan, F. Malik, P. Lee, S. Lee, S.V. Springham, T.L. Tan, M. Krishnan, R.S. Rawat, Plasma Sources Sci. Technol. 17 (2008) 045020.
[11] R.K. Rout, P. Mishra, A.M. Rawool, L.V. Kulkarni, S.C. Gupta, J. Phys. D: Appl. Phys. 41 (2008) 205211.
[12] P. Silva, J. Moreno, L. Soto, L. Birstein, R.E. Mayer, W. Kies, Appl. Phys. Lett. 83 (2003) 3269.
[13] M. Milanese, R. Moroso, J. Pouzo, Eur. Phys. J. D 27 (2003) 77.
[14] L. Soto, P. Silva, J. Moreno, M. Zambra, W. Kies, R.E. Mayer, A. Clausse, L. Altamirano, C. Pavez, L. Huerta, J. Phys. D: Appl. Phys. 41 (2008) 205215.
[15] L. Soto, C. Pavez, P. Silva, J. Moreno, M. Barbaglia, A. Clausse, Plasma Sources Sci. Technol. 18 (2009) 015007.
[16] J. Moreno, L. Birstein, R.E. Mayer, P. Silva, L. Soto, Meas. Sci. Technol. 19 (2008) 087002.
[17] M.G. Haines, Philos. Trans. R. Soc. London A 300 (1981) 649.
[18] H. Schmidt, M. Sadowski, L. Jakubowski, E.S. Sadowska, J. Stanislawski, Plasma Phys. Control. Fusion 36 (1994) 13.
[19] D.E. Potter, Phys. Fluids 14 (1971) 1911.
[20] G.J. Pert, J. Phys. D: Appl. Phys. 1 (1968) 1487.
[21] M.A.M. Kashani, T. Miyamoto, AIP Conf. Proc. 651 (2002) 249.
[22] L.H. Li, H.Q. Zhang, J. Phys. D: Appl. Phys. 29 (1996) 2217.
[23] S. Lee, S.H. Saw, Appl. Phys. Lett. 92 (2008) 021503.
[24] S. Lee, P. Lee, S.H. Saw, R.S. Rawat, Plasma Phys. Control. Fusion 50 (2008) 065012.
[25] S. Lee, S.H. Saw, J. Fusion Energy 27 (2008) 292.
[26] http://www.intimal.edu.my/school/fas/UFLF/File7RADPF05.13.9b.xls.